9th AUSTRALASIAN
FLUID MECHANICS CONFERENCE
AUCKLAND, 8-12 DECEMBER 1986

Numerical Solution for the Flow of Viscoelastic Fluids around an Inclined Circular Cylinder

K. CHIBA and A. HORIKAWA

Department of Mechanical Engineering, Osaka University, Osaka, Japan.

ABSTRACT

Finite difference solutions have been obtained by the perturbation method to investigate the influence of shear thinning and elasticity on the flow around an inclined circular cylinder of finite length and the hydrodynamic force. The upper-convected Maxwell model, in which the viscosity changes according to Cross model, has been used. Viscoelastic fluids are prone to flow axially in the vicinity of a cylinder. The numerical predictions generally agree with the flow visualization results. The numerical solutions also show that elasticity has a strong effect on the flow profile especially around both ends of the cylinder. When only shear thinning is taken into account, the moment acts on the cylinder in the way so as to rotate it into a perpendicular orientation to the incoming flow, whereas the moment to rotate the cylinder into a parallel orientation to the flow can be obtained when both shear thinning and elasticity are taken into account.

1 INTRODUCTION

A slender body, namely a straight circular cylinder with a large length to diameter ratio, falling in quiescent Newtonian liquids rotates to adopt a horizontal orientation, whereas it rotates towards a vertical orientation when falling through quiescent polymer solutions(Chiba et al., 1986). This phenomenon depends strongly on shear thinning and elasticity, however, it is still not clear how the viscoelasticity contributes to the attitude variation of the body. It is necessary to study and discuss closely the velocity and stress fields of viscoelastic fluids around a circular cylinder inclined to the flow.

A few papers have been published on the three-dimensional flow of Newtonian fluids around an inclined circular cylinder of finite length in a uniform flow. Slauti & Gerrard(1981) and Ramberg(1983) dealt with the dependence of the configuration of the vortices on various end constructions but they did not study quantitatively the three-dimensional flow. To our knowledge, there are no existing data, either theoretical or experimental, on viscoelastic flow around a finite cylinder.

In this paper, numerical solutions are presented for the flow around an inclined circular cylinder of finite length and the hydrodynamic force in a uniform flow of Newtonian, non-Newtonian inelastic and viscoelastic fluids, and the influence of shear thinning and elasticity is discussed. The particle path predictions around the cylinder are also compared with the flow visualization results obtained using dye injection method.

2 BASIC THEORY

Motion of incompressible continua obey the following equations:

Equation of continuity; $$v^i{}_{,i} = 0 \qquad (1)$$

Cauchy's equation of motion; $$\rho D v^i / D t = -p_{,j} g^{ij} + T^{ij}{}_{,j} \qquad (2)$$

where v^i;velocity vector, ρ;liquid density, p;isotropic pressure, T^{ij};extra stress tensor, g^{ij};metric tensor, and D/Dt;material derivative.

The upper-convected Maxwell model in which the viscosity changes according to Cross model(1965) is used. The constitutive equations are given by

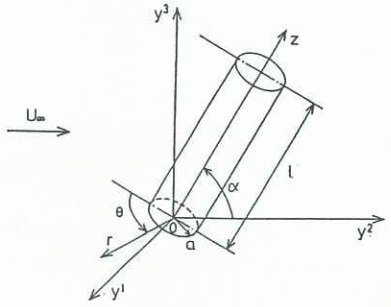

Figure 1 The coordinate system.

$$(1+\lambda D_0/Dt)\,T^{ij} = 2\,\Theta e^{ij} \qquad (3)$$

and viscosity Θ is

$$\Theta = \eta_\infty + (\eta_0 - \eta_\infty)/[1+\kappa(4|II_e|)^{1/3}] \qquad (4)$$

where η_0;zero-shear viscosity, η_∞;infinite-shear viscosity, κ;material prameter, e^{ij};deformation rate tensor of Euler, II_e;second invariant of e^{ij}, λ;relaxation time ,and D_0/Dt;convected derivative.

We consider the steady flow past a circular cylinder of radius,a, and of length,l, as shown in Figure 1. At infinity the fluid is assumed to flow in the y^2 direction with a constant velocity U_∞. We refer all motion to a set of cylindrical polar coordinates(r,θ,z), where the z axis is inclined to the y^2 axis at an angle of α in the y^2y^3 plane. We introduce a vector potential ψ defined by $\mathbf{v}=\mathrm{curl}\psi$. The equation of continuity is satisfied identically. We make a transformation into non-dimensional variables as follows:

$$r^*=r/a,\ z^*=z/a,\ v_r^*=v_r/U_\infty,\ v_\theta^*=v_\theta/U_\infty,\ v_z^*=v_z/U_\infty,\ p^*=p/(\rho U_\infty^2/2),$$
$$T_{rr}^*=T_{rr}/(\eta_0 U_\infty/a),\ T_{\theta\theta}^*=T_{\theta\theta}/(\eta_0 U_\infty/a),\ T_{zz}^*=T_{zz}/(\eta_0 U_\infty/a),$$
$$T_{r\theta}^*=T_{r\theta}/(\eta_0 U_\infty/a),\ T_{\theta z}^*=T_{\theta z}/(\eta_0 U_\infty/a),\ T_{zr}^*=T_{zr}/(\eta_0 U_\infty/a),\ \psi_r^*=\psi_r/aU_\infty, \qquad (5)$$
$$\psi_\theta^*=\psi_\theta/aU_\infty,\ \psi_z^*=\psi_z/aU_\infty,\ \omega_r^*=\omega_r/(U_\infty/a),\ \omega_\theta^*=\omega_\theta/(U_\infty/a)\ \omega_z^*=\omega_z/(U_\infty/a),$$
$$\tau=t/(a/U_\infty),\ Re=2a\rho U_\infty/\eta_0,\ We=\lambda U_\infty/2a,\ l^*=l/a$$

where Re;Reynolds number, We;Weissenberg number.

We eliminate the isotropic pressure from the three equations of motion to get the vorticity transport equations . The vorticity vector ω^* is also related to the vector potential ψ^*. For brevity, thses equations are not written here. The boundary conditions on velocity components are at infinity;

$$v_r^* = -\sin\alpha\cos\pi\eta\ ,\ v_\theta^* = \sin\alpha\sin\pi\eta\ ,\ v_z^* = \cos\alpha \qquad (6)$$

on the cylinder; $$v_r^* = v_\theta^* = v_z^* = 0 \qquad (7)$$

and in the symmetric plane; $$\partial v_r^*/\partial\eta = \partial v_z^*/\partial\eta = v_\theta^* = 0 \qquad (8)$$

Our purpose is to analyze the flow when the elastic effect begins to appear. So, such a assumption can be introduced as We<1. Then, the numerical analysis is carried out as a perturbation expansion in the small Weissenberg number. For the two-dimensional viscoelastic flow past a circular cylinder, the contribution of the second order stress of the Weissenberg number to the total drag force is at most 2 or 3%. So, we take into account only the zero and first order terms in the present computations. The zero order term show a non-Newtonian inelastic flow.

The ADI method is used to calculate the values of the vorticity at the new time step and the solutions of the

Table 1 Calculation conditions for Newtonian and non-Newtonian inelastic fluids.

fluid	Re	$\alpha(°)$	d(mm)	l^*	$\Delta\tau$
Newtonian fluid	0.1	45	5	40	0.5×10^{-4}
	1				0.5×10^{-3}
	10				0.5×10^{-2}
	10	15			0.5×10^{-2}
	10	75			
non-Newtonian Fluid 1	1	45	5	40	0.5×10^{-3}
	10				0.5×10^{-2}
	1	45	2		0.5×10^{-3}
	10				0.5×10^{-2}
	1	15	2		0.5×10^{-3}
		75			
non-Newtonian Fluid 2	1	75	2	40	0.5×10^{-3}

Fluid 1 : $\eta_0=0.03527$ (Pa·s), $\eta_\infty=0.00256$ (Pa·s), $\kappa=0.1871$
Fluid 2 : $\eta_0=0.1005$ (Pa·s), $\eta_\infty=0.00240$ (Pa·s), $\kappa=0.4914$

Table 2 Calculation conditions for viscoelastic fluids.

shear thinning	Re	$\alpha(°)$	d(mm)	l^*	$\Delta\tau$
Fluid 1	1	15	2	40	0.4×10^{-3}
		75			
Fluid 2	1	75	2	40	0.4×10^{-3}

Vector potential equations are obtained by the SOR method . The ADI method divides the time step $\Delta\tau$ into three one third steps,$\Delta\tau/3$. The computational conditions are listed in Tables 1 and 2. We use two kinds of shear thinning behaviors termed non-Newtonian Fluid 1 and 2 in Figure 2. Each behavior corresponds to that of 0.05wt% and 0.1wt% Separan AP-30 solutions, respectively. The computational domain and grid size are as follows: $0\leq\eta\leq1$, $\Delta\eta=1/12$; $\xi\leq1.2$, giving an outer non-dimensional radius r_∞^* of 43.4, $\Delta\xi=0.1$; $-20\leq\zeta\leq60$, $\Delta\zeta=2.5$. Where the following transformation of the independent variables is made

$$r^*=e^{\pi\xi}\ ,\quad \eta=\theta/\pi\ ,\quad \zeta=z^* \tag{9}$$

3 PARTICLE PATH AND VELOCITY FIELD AROUND THE CYLINDER

Particle path can be obtained by moving a particle at the same velocity as fluid velocity from twenty three initial positions (r_0^*,θ_0,z_0^*). It is three-dimensional curve, so we mainly draw its projection onto the symmetric plane ,$\theta=0,\pi$, to compare it with the streak lines obtained by the flow visualization experiments which are conducted by injecting methylene blue dye solution slowly through the small holes provided on the cylindrical surface and end face. A circular cylinder of 5 mm in diameter and 200 mm in length is used and the dye streak lines are photographed.

From dye streak lines in Figures 3(b) and 3(c), the local flow over the cylinder is only slightly deflected. However in the wake flow the streak lines are remarkably influenced by the axial flow and rapidly flow up parallel to the axis. Then they gradually rejoin direction of the incoming flow. In figure 3(a), it can be seen that the particle paths become closer to the incoming flow direction for the non-Newtonian inelastic fluid than for the Newtonian fluid as the cylinder is approached; fluids with the shear thinning viscosity are prone to flow axially in the vicinity of the cylinder. This is because the shear thinning behavior greatly reduces the fluid viscosity adjacent to the cylinder. This tendency is verified by measuring the angles of the streak lines against the cylinder's axis at $\theta=90°$ on the streak line photographs.

Figure 3 shows that the dye flows up parallel to the axis behind the cylinder because it enters the wake region , whereas this phenomenon can not be predicted because the particle moves over this region. The particle paths in the wake flow are shown in Figure 4 for the non-Newtonian Fluid 1. The particles flow towards the leeward end accompanied by spiralling and the rapid flow-up phenomenon similar to that of the observed streak lines when moving away from the cylinder can be seen.

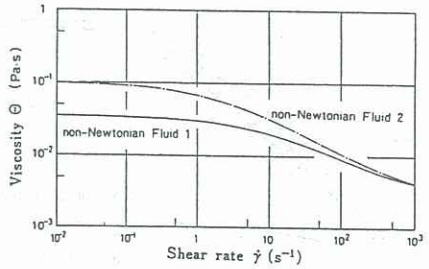

Figure 2 Shear thinning viscosity used in calculations.

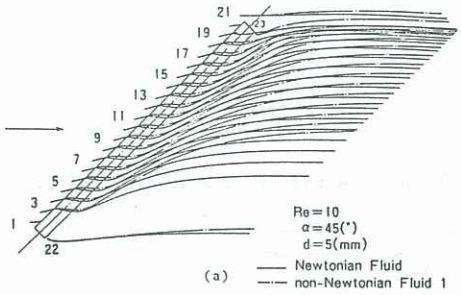

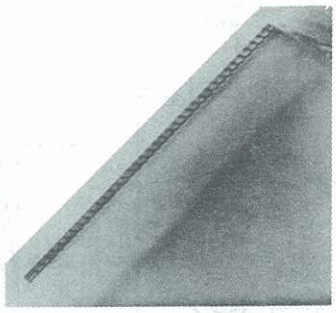

(b)

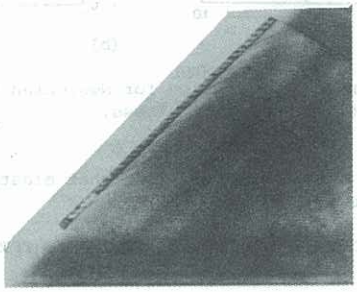

(c)

Figure 3 Particle path around a cylinder, (a)particle path for Newtonian fluid and non-Newtonian inelastic fluid, $r_0^*=2$, $\theta_0=5°$, (b)dye streak lines in water, Re=9.7 , (c)dye streak lines in a 0.05wt% Separan AP-30 solution , Re=10.

Let us now consider the influence of elasticity on the velocity field. We plot velocity profiles on the cylindrical surface of $\xi=0.1$ in Figure 5. If one introduce elasticity into the fluid, then both v_θ^* and v_z^* of the non-Newtonian inelastic fluid increase in the front zone and, in reverse, decrease in the rear zone. The profiles of the first order velocities of the Weissenberg number, $v_\theta^{(1)}$ and $v_z^{(1)}$, show that the differences in $v_\theta^{(1)}$ and $v_z^{(1)}$ between at the symmetric positions about the cylinder's center of mass are small in a mid region of the cylinder, however, they become considerably large as both ends are approached. This indicates that the elastic effect manifests itself remarkably in the region where the velocity field changes drastically. Figure 5(a) shows that elasticity decreases the difference in v_θ^* between at the windward end and at the leeward end. In addition, for the non-Newtonian inelastic fluid the axial velocity v_z^* gradually forms a symmetric profile with respect to $\eta=0.5$ towards the leeward end in Figure 5(b). However, such a symmetric profile of v_z^* can not be seen for the viscoela-

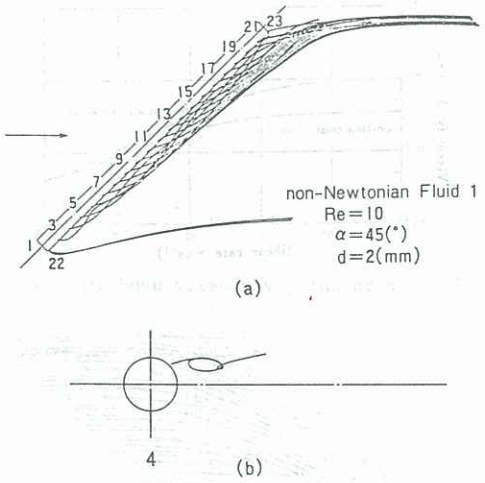

Figure 4 Particle path in a wake flow, $r_0^*=1.1$, $\theta_0=135°$.

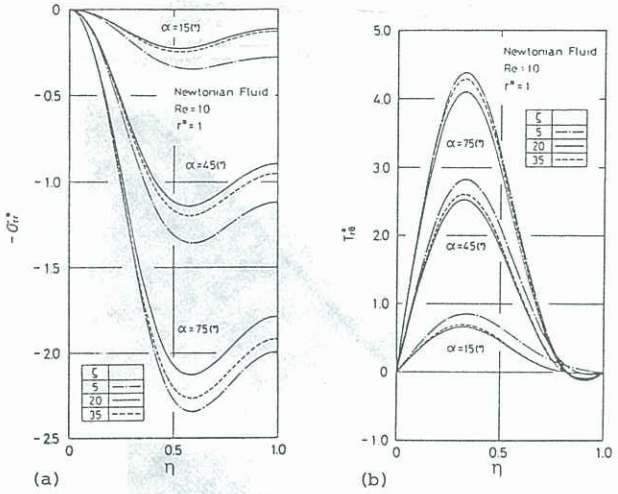

Figure 6 Stress distribution for Newtonian fluid, (a) normal stress, (b) shear stress.

stic fluid. It also seems clear that elasticity increases the asymmetry of v_θ^*.

4 STRESS DISTRIBUTION AND HYDRODYNAMIC FORCE ON THE CYLINDER

The cylinder is subject to a drag force in each of the perpendicular and axial directions, D_p and D_a, and a moment, N. To compute these, we must calculate the distributions of normal stress and shear stress around the surface of the cylinder. The extra stress components are obtained from the constitutive equations and the isotropic pressure distribution around the cylindrical surface is found by integrating the θ momentum equation. The stresses for viscoelastic fluids are given by, e.g.

$$[\sigma_{rr}^*]_{\xi=0} = [\sigma_{rr}^{(0)} + \sigma_{rr}^{(1)} We]_{\xi=0} \qquad (10)$$

In Figures 6 and 7, we plot the normal stress, σ_{rr}^*, and shear stress, $T_{r\theta}^*$, distributions at three different positions, i.e. at ζ=5, 20 and 35. For both Newtonian and non-Newtonian inelastic fluids, σ_{rr}^* and $T_{r\theta}^*$ are minimum at ζ=20 and maximum at ζ=5. The shear thinning behavior greatly reduces the fluid viscosity adjacent to the cylnder, in turn reduces σ_{rr}^* and $T_{r\theta}^*$ of the Newtonian fluid . When a fluid flows around an inclined cylinder, the axial flow varies the shear rate on the cylinder surface along the axis and the shear rate near the leeward end becomes smaller than that near the windward end. For non-Newtonian inelastic fluids, an increase in viscosity compensates to some extent for a decrease in the velocity gradient, so the differences in σ_{rr}^* and $T_{r\theta}^*$ between at ζ=5 and ζ=35 become smaller compared with for Newtonian fluids.

Both the first order normal stress and shear stress of

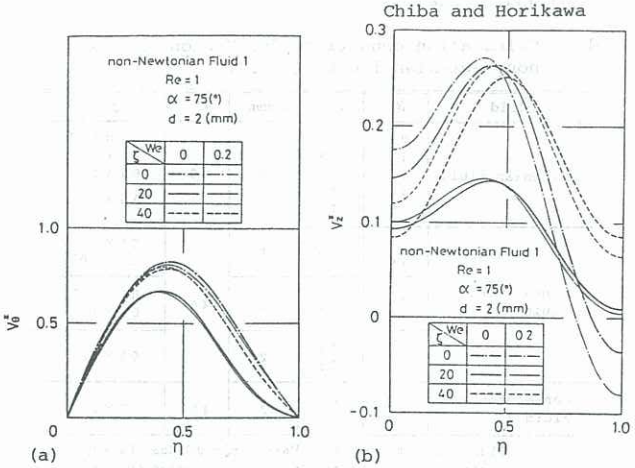

Figure 5 Velocity profile for non-Newtonian inelastic fluid and viscoelastic fluid, (a) circumferential velocity, (b) axial velocity.

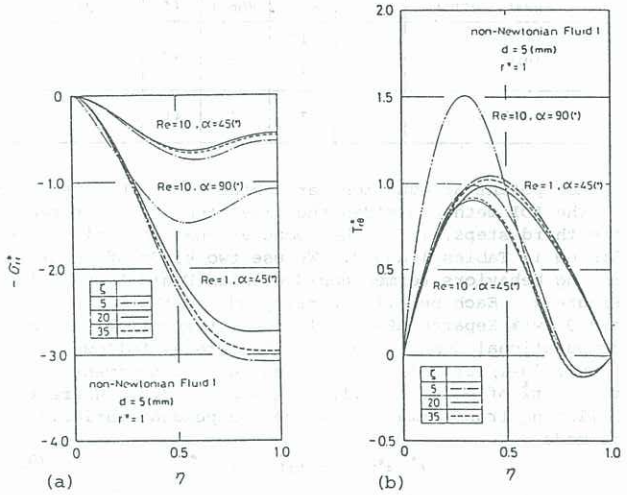

Figure 7 Stress distribution for non-Newtonian inelastic fluid, (a) normal stress, (b) shear stress.

the Weissenberg number, $\sigma_{rr}^{(1)}$ and $T_{r\theta}^{(1)}$, show a similar tendency to that of the first order velocity; the differences in $\sigma_{rr}^{(1)}$ and $T_{r\theta}^{(1)}$ between at the symmetric positions about the cylinder's center of mass are small in a mid region of the cylinder, however, they become considerably large as both ends are approached. As might be expected, the elastic effect on the stress distributions appear markedly in the region where elasticity has a strong effect on the velocity field. The fact that $\sigma_{rr}^{(1)}$ is about a hundred times larger than $T_{r\theta}^{(1)}$ leads to the conclusion that elasticity has little effect on the shear stress, whereas it strongly affects the normal stress. In Figure 8(a), for the non-Newtonian inelastic fluid the normal stress is positive around the cylindrical surface, whereas it becomes negative in the front zone of the cylinder as the elasticity increases. The reason for this is that stream near the cylinder is deflected around the surface and, as a result, a compressive force due to the elastic force acts in the front zone for viscoelastic fluids.

We now discuss the hydrodynamic force. The drag forces vary along the cylinder's axis. Let $\Delta D_{rr}^*, \Delta D_{r\theta}^*$ denote the perpendicular drag forces per unit length due to σ_{rr} and $T_{r\theta}$, respectively, and ΔD_{zr}^* the axial drag force due to T_{zr}. They are normalized with respect to $\pi a \rho U_\infty^2/2$. ΔD_{rr}^*, $\Delta D_{r\theta}^*$ and ΔD_{zr}^* rise to a peak near both ends of the cylinder, but then fall rapidly as a mid region is approached. Especially ΔD_{rr}^* and $\Delta D_{r\theta}^*$ keep almost constant along the cylinder's axis in the mid region, $10<\zeta<30$.

The effect of shear thinning and elasticity on the drag force as follows: the shear thinning behavior decreases both perpendicular and axial drag forces, and also decreases the difference between the perpendicular drag force near the windward end and that near the leeward end.

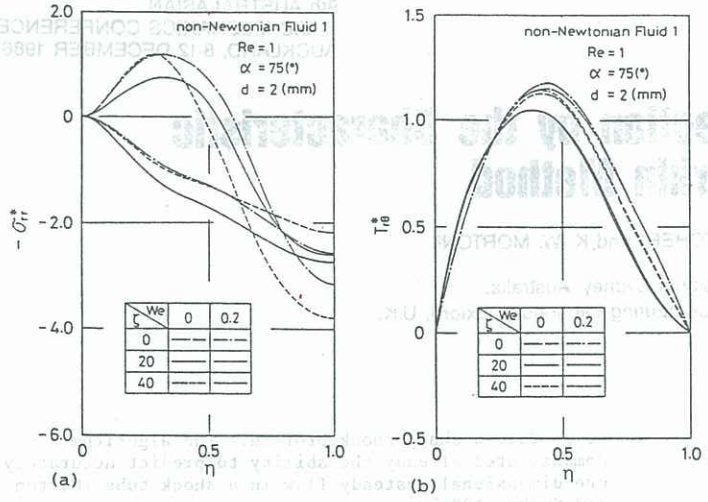

Figure 8 Stress distribution for non-Newtonian inelastic fluid and viscoelastic fluid, (a)normal stress, (b)shear stress.

Elasticity increases ΔD^*_{rr}. Because an increment in ΔD^*_{rr} near the leeward end is larger than that near the windward end, the former drag force exceeds the latter one as the Weissenberg number increases. $\Delta D^*_{r\theta}$ and ΔD^*_{zr}, however, are little influenced by elasticity.

The moment, N, round the cylinder's center of mass is due to ΔD^*_{rr}, $\Delta D^*_{r\theta}$ and the frictional drag forces on the end faces. Its sign is defined to be positive when the moment acts in such a way as to rotate the cylinder into a perpendicular orientation to the incoming flow. Let N^* denote the moment normalized with respect to $\pi a^3 \rho U_\infty^2/2$. To investigate the contribution of the distributions of ΔD^*_{rr} and $\Delta D^*_{r\theta}$ to a moment, N^*, we plot ΔN^* distribution in Figure 9, which is given in the following form.

$$\Delta N^* = [(\Delta D_{rr}^* + \Delta D_{r\theta}^*)_\zeta - (\Delta D_{rr}^* + \Delta D_{r\theta}^*)_{l^*-\zeta}](l^*/2 - \zeta) \quad (11)$$

For the non-Newtonian inelastic fluid ΔN^* is positive over a range of ζ, but ΔN^* at ζ=0 falls to a negative value with an increase in elasticity. And ΔN^* becomes negative even at ζ=2.5 for We=0.3. Figure 9, thus, shows that the moment is due to the difference in perpendicular drag force between $0<\zeta<10$ and $30<\zeta<40$.

D^*_p, D^*_a, the total perpendicular and axial drag forces normalized with respect to $\pi a^2 \rho U_\infty^2/2$, and N^* are listed in Table 3. Tables 3(a) and 3(b) show that the moment, N, increases with the incoming flow velocity for both Newtonian and non-Newtonian inelastic fluids. From Table 3 (b), when only shear thinning is taken into account, the moment acts in the way so as to rotate the cylinder into a perpendicular orientation to the flow. However, the shear thinning behavior decreases the Newtonian moment and the moment also decreases with increasing shear thinning. On the other hand, Table 3(c) shows that N^* decreases as the Weissenberg number increases, and it becomes negative at the Weissenberg number equal to about 0.2 for the non-Newtonian Fluid 2 and α=75°. From above discussion, we can obtain an important conclusion that the moment acts to rotate the cylinder into a parallel orientation to the flow when both shear thinning and elasticity are taken into account.

5 CONCLUSIONS

1. The local flow over the cylinder is only slightly deflected. However, the particle path rapidly flows up parallel to the cylinder's axis in the wake flow. Then it gradually rejoins direction of the incoming flow. The numerical predictions generally agree with the flow visualization results.
2. Elasticity has a particularly strong effect on the velocity field in the region where the velocity changes drastically, i.e. region near both ends of the cylinder.
3. For Newtonian and non-Newtonian inelastic fluids, the moment, which acts in the way so as to rotate the cylinder into a perpendicular orientation to the flow, increases with an increase in the Reynolds number.

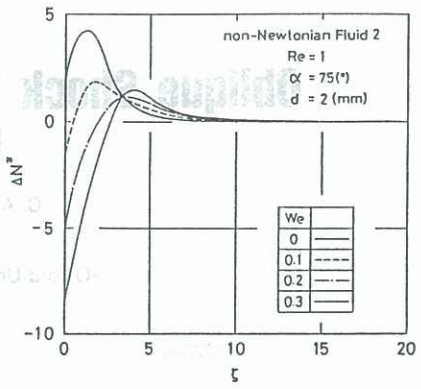

Figure 9 Contribution of drag force distribution to moment.

Table 3 Calculated drag forces and moment.
(a)for Newtonian fluid

α(°)	Re	l^*	D_p^*	D_a^*	N^*
45	0.1	40	3157	1850	296.6
	1		320.6	187.0	103.5
	10		50.43	27.08	64.32
15	10		12.09	28.56	41.75
75	10		86.38	11.85	28.69

(b)for non-Newtonian inelastic fluid

shear thinning	α(°)	Re	d (mm)	l^*	D_p^*	D_a^*	N^*
Fluid 1	45	1	5	40	238.6	140.9	79.19
		10	5		20.45	16.13	30.48
		1	2		141.1	95.44	54.38
		10	2		17.21	12.47	47.91
	15	1	2	40	58.09	141.3	89.43
	75	1	2	40	217.1	42.50	40.31
Fluid 2	75	1	2	40	63.59	13.20	11.31

(c)for viscoelastic fluid

shear thinning	α(°)	Re	d (mm)	l^*	We	D_p^*	D_a^*	N^*
Fluid 1	15	1	2	40	0.1	57.91	141.2	75.03
					0.2	57.73	141.0	60.62
					0.3	57.55	140.9	46.21
	75	1	2	40	0.1	225.4	42.32	28.39
					0.2	233.6	42.14	16.47
					0.3	241.9	41.96	4.544
Fulid 2	75	1	2	40	0.1	66.34	13.14	5.868
					0.2	69.08	13.08	0.4256
					0.3	71.82	13.01	−5.017

4. The shear thinning behavior greatly reduces the fluid viscosity adjacent to the cylinder, in turn reduces drag force. In addition, an increase in viscosity compensates to some extent for a decrease in the velocity gradient on the cylinder surface. Therefore, the moment to rotate the cylinder into a perpendicular orientation to the flow decreases with an increase in shear thinning.
5. Elasticity has little effect on shear stress, whereas it strongly affects normal stress and the drag force due to the normal stress becomes larger as elasticity increases. This elastic effect is especially remarkable near both ends of the cylinder.
6. When only shear thinning is taken into account, the moment acts in the way so as to rotate the cylinder into a perpendicular orientation to the flow. In contrast, the moment to rotate the cylinder into a parallel orientation to the flow can be predicted when both shear thinning and elasticity are taken into account.

REFERENCES

Chiba, K;Song, K;Horikawa, A (1986): Rheol. Acta,in press
Cross, M M (1965): J. Coll. Sci., 20, 417-437
Ramberg, S E (1983): J. Fluid Mech., 128, 81-107
Slaouti, A;Gerrard, J H (1981): ibid., 112, 297-314